

# Wideband Array Processing Using Total Least-Squares Transformations

S. Valaee<sup>1,2</sup> and P. Kabal<sup>1,2</sup>

<sup>1</sup>Elect. Eng., McGill University, Montreal, Quebec, CANADA H3A 2A7

<sup>2</sup>INRS-Télécommunications, Verdun, Quebec, CANADA H3E 1H6

## Abstract

In this paper, we introduce a new technique for wideband array processing. The new algorithm is based on the total least-square approach. The total least-square method is an alternative to the least-square method and uses the fact that the errors can exist both in the focusing location matrix and the estimated location matrix at the frequency bin. To prevent the focusing loss, we use a unitary approach for focusing. The new method does not require singular value decomposition. The computational complexity for the new technique is significantly lower than that for the similar methods which use singular value decomposition. The simulation results show that the new algorithm has a smaller resolution signal-to-noise ratio than the coherent signal-subspace method. The bias in the estimation of the directions-of-arrival is also smaller for the new method than that for the coherent signal-subspace method.

## 1. Introduction

Recent literature in array processing show a growing interest in the analysis of wideband signals [1] [2] [3]. Wideband array processing arises in many applications such as passive sonar, microphone array for teleconferencing and spread spectrum. Several approaches have been taken in the literature to process wideband signals. Some methods sample the frequency spectrum to create narrowband signals. In these methods, the output of the sensors are separated into nonoverlapping snapshots. In each snapshot a DFT algorithm is used to sample the spectrum in the frequency domain. At each frequency bin a narrowband signal is formed which has the same directions-of-arrival (DOAs) of the wideband sources. In the coherent signal-subspace method (CSM) [1] the correlation matrices at different frequency bins are combined to form a universal correlation matrix. This universal correlation matrix is a sufficient statistic for the observation vectors [4]. Then, a high resolution algorithm, such as MUSIC, is applied to estimate the DOAs. In CSM, the combination of the narrowband samples is done through transformation of the observation

vectors. This is called *focusing*. The focusing operator is a matrix that transforms the location matrix of the array at a sampling frequency to the location matrix at the focusing frequency. It has been shown that the CSM algorithm can resolve coherent sources.

An improved version of the CSM is also reported in the literature that uses unitary focusing matrices [2]. The unitary transformation does not create a *focusing loss*. The unitary focusing matrices are determined based on a least-square (LS) minimization between the transformed location matrix at each frequency bin and the focusing location matrix.

In this paper, we introduce a total least-square (TLS) formulation of the coherent signal subspace techniques. The TLS is known to provide unbiased solution where both the model and the observations are noisy; a property which does not hold for the least square solution [5].

## 2. Coherent wideband processing

Suppose  $q$  wideband sources are arriving at an array of  $p$  sensors from the distinct angles  $\theta_i$ ,  $i = 1, \dots, q$ , made with the broadside of the array. The output of the sensors are observed in  $T$  seconds and decomposed into  $N$  snapshots of  $\Delta T$  duration such that  $N\Delta T = T$ . A  $J$ -point FFT algorithm is used in each snapshot to sample the spectrum of the signals. The observation vector at the output of the sensors at the frequency bin  $\omega_j$  is given by

$$\mathbf{x}(\omega_j) = \mathbf{A}(\omega_j, \theta)\mathbf{s}(\omega_j) + \mathbf{n}(\omega_j) \quad (1)$$

where  $\mathbf{x}(\omega_j)$ ,  $\mathbf{s}(\omega_j)$  and  $\mathbf{n}(\omega_j)$  are the Fourier transforms of the observation, signal and noise vectors, and  $\mathbf{A}(\omega_j, \theta) = [\mathbf{a}(\omega_j, \theta_1) \dots \mathbf{a}(\omega_j, \theta_q)]$  is the  $p \times q$  location matrix. It is assumed that  $\mathbf{A}(\omega_j, \theta)$  is full rank. In other words, for each  $\omega_j$  the steering vectors  $\mathbf{a}(\omega_j, \theta_i)$  are linearly independent.

Temporal samples of the signals and noise are considered to be independent circular-Gaussian distributed. It is further assumed that the noise is spatially white. A non-white case can also be handled with the proposed method as long as the spatial correlation of the noise is known but for a scalar multiplier. The correlation matrices of the signal and noise at the  $j$ -th frequency bin are represented by  $\mathbf{S}(\omega_j)$  and  $\sigma^2(\omega_j)\mathbf{I}$ , respectively. For a large  $\Delta T$ , samples of

This work is supported by a grant from the Natural Sciences and Engineering Research Council of Canada (NSERC)

the observation vector at different frequency bins are uncorrelated and the correlation matrix of the array at the  $j$ -th frequency bin can be written as

$$\mathbf{R}(\omega_j) = \mathbf{A}(\omega_j, \theta) \mathbf{S}(\omega_j) \mathbf{A}^H(\omega_j, \theta) + \sigma^2(\omega_j) \mathbf{I} \quad (2)$$

where the superscript  $H$  represents the Hermitian transpose. For simplicity of notation we suppress the frequency variable and show the frequency dependence only by the subscript  $j$ . The universal correlation matrix in the CSM algorithm can be shown as

$$\mathbf{R} = \sum_{j=1}^J \mathbf{T}_j \mathbf{A}_j \mathbf{S}_j \mathbf{A}_j^H \mathbf{T}_j^H + \sum_{j=1}^J \sigma_j^2 \mathbf{T}_j \mathbf{T}_j^H \quad (3)$$

where  $\mathbf{T}_j$  is the  $j$ -th focusing matrix.

In [2] a unitary version of the CSM algorithm is introduced which is based on choosing  $\mathbf{T}_j$  to

$$\begin{aligned} \min \|\mathbf{A}_0 - \mathbf{T}_j \mathbf{A}_j\|^2, \quad j = 1, \dots, J \\ \text{s.t.} \quad \mathbf{T}_j^H \mathbf{T}_j = \mathbf{I} \end{aligned} \quad (4)$$

where  $\mathbf{A}_0$  is the focusing location matrix of the array and  $\|\cdot\|$  is the Frobenius norm of a matrix. The matrix  $\mathbf{T}_j$  that solves (4) is the focusing matrix of the unitary CSM algorithm. Multiplication of  $\mathbf{T}_j$  by  $\mathbf{A}_j$  transforms the signal subspace at the  $j$ -th frequency bin into the focusing signal subspace. It has been shown that the unitary CSM does not create focusing loss [2]. The focusing loss is defined as the ratio of the signal-to-noise ratio after focusing to the signal-to-noise ratio before focusing.

To determine the focusing matrix  $\mathbf{T}_j$  from (4), it is assumed that the matrices  $\mathbf{A}_j$  and  $\mathbf{A}_0$  are known. In practice, an ordinary beamformer is applied to estimate the DOAs of the sources. If the distance between the sources is smaller than the beamwidth of the beamformer, the spatial spectrum will display a single peak in the vicinity of the actual sources. The location of the detected peak serves as a pre-estimated DOA for focusing. In practice, a few more focusing angles are added in the vicinity of the pre-estimated DOA [2]. The focusing angles are used to determine the  $p \times \hat{q}$  location matrices  $\mathbf{A}_0$  and  $\mathbf{A}_j$  where  $\hat{q}$  is the number of the focusing DOAs.

### 3. The TLS algorithm

In this section, we derive a total least-square coherent signal-subspace method for wideband array processing. The least-square problem (4) can be rearranged as

$$\begin{aligned} \min_{\mathbf{T}_j} \|\mathbf{E}_0\|^2 \\ \text{s.t.} \quad \mathbf{A}_0 + \mathbf{E}_0 = \mathbf{T}_j \mathbf{A}_j \\ \mathbf{T}_j^H \mathbf{T}_j = \mathbf{I} \end{aligned} \quad (5)$$

where  $\mathbf{E}_0$  is a perturbation matrix. The constraints in this minimization problem show that the location matrix  $\mathbf{A}_0$  is perturbed such that  $\mathbf{A}_j$  can be transformed onto it using a unitary matrix. The minimization (5) guarantees that the

perturbation matrix has the smallest Frobenius norm. The following lemma proves that the perturbation matrix  $\mathbf{E}_0$  is in the same subspace as the location matrix  $\mathbf{A}_0$ . Thus the perturbation matrix needs to be searched for only in the subspace spanned by the columns of  $\mathbf{A}_0$ .

**Lemma 1.** *The perturbation matrix  $\mathbf{E}_0$  which minimizes (5) and the location matrix  $\mathbf{A}_0$  in (5) span the same subspace.*

The proofs for the lemmas and the theorems of this paper can be found in [6].

In a total least-square approach, both  $\mathbf{A}_0$  and  $\mathbf{A}_j$  are perturbed. The total least-square formulation is given by

$$\begin{aligned} \min \|\mathbf{F}_0 \mathbf{F}_j\|^2 \\ \text{s.t.} \quad \mathbf{A}_0 + \mathbf{F}_0 = \mathbf{T}_j (\mathbf{A}_j + \mathbf{F}_j) \\ \mathbf{T}_j^H \mathbf{T}_j = \mathbf{I} \end{aligned} \quad (6)$$

where  $\mathbf{F}_0$  and  $\mathbf{F}_j$  are the perturbation matrices. Note that (6) is slightly different from the classical total least-square formulation. In the classical total least-square approach the system of equations is over-determined and it is assumed that in an unperturbed case, a consistent solution exists for the over-determined set of equations. However, the first constraint of (6) indicates an under-determined set of equations with a unitary solution matrix. Furthermore, no unitary  $\mathbf{T}_j$  can solve  $\mathbf{A}_0 = \mathbf{T}_j \mathbf{A}_j$  unless  $\mathbf{A}_0$  and  $\mathbf{A}_j$  have the same set of singular values and right singular vectors. Also for the classical total least-squares problem, a unitary constraint produces the same results as the least-squares formulation [7].

**Theorem 1.** *The perturbation matrices in the total least-square approach are in the same subspaces as the location matrices. In other words,  $\mathbf{F}_0$  and  $\mathbf{A}_0$  span the same subspace, and similarly  $\mathbf{F}_j$  and  $\mathbf{A}_j$  span the same subspace.*

**Theorem 2.** *Assume that the polar decomposition of the  $p \times \hat{q}$  matrices  $\mathbf{A}_0$  and  $\mathbf{A}_j$  are shown by  $\mathbf{W}_0 \mathbf{Q}_0$  and  $\mathbf{W}_j \mathbf{Q}_j$ , where  $\mathbf{W}_0$  and  $\mathbf{W}_j$  are  $p \times \hat{q}$  matrices with orthogonal columns, and  $\mathbf{Q}_0$  and  $\mathbf{Q}_j$  are  $\hat{q} \times \hat{q}$  Hermitian positive-definite matrices. Then, the perturbation matrices*

$$\mathbf{F}_0 = \frac{1}{2} \mathbf{W}_0 (\mathbf{Q}_j - \mathbf{Q}_0) \quad (7)$$

$$\mathbf{F}_j = \frac{1}{2} \mathbf{W}_j (\mathbf{Q}_0 - \mathbf{Q}_j) \quad (8)$$

satisfy (6) with the transformation matrix  $\mathbf{T}_j$  given by

$$\mathbf{T}_j = \mathbf{U}_0 \mathbf{U}_j^H \quad (9)$$

where  $\mathbf{U}_0$  and  $\mathbf{U}_j$  are any orthonormal matrices with the first  $\hat{q}$  columns equal to  $\mathbf{W}_0$  and  $\mathbf{W}_j$ .

If the number of focusing angles is smaller than the number of sensors, the rank of  $\mathbf{A}_0$  and  $\mathbf{A}_j$  is not equal to  $p$  and the unitary solution (9) is not unique. However, for DOA estimation, it suffices to multiply those singular vectors of  $\mathbf{A}_0$  and  $\mathbf{A}_j$  that correspond to the nonzero singular values.

In such a case,  $\mathbf{T}_j$  is not unitary, but it has  $\hat{q}$  nonzero singular values equal to 1. Thus, the constraint  $\mathbf{T}_j^H \mathbf{T}_j = \mathbf{I}$  can be substituted with  $\sigma_i(\mathbf{T}_j) = 1$ , for  $i = 1, \dots, \hat{q}$ , and  $\sigma_i(\mathbf{T}_j) = 0$ , for  $i = \hat{q} + 1, \dots, p$ , where  $\sigma_i(\mathbf{T}_j)$  is the  $i$ -th singular value of  $\mathbf{T}_j$ . In such a case the solution to Theorem 2 is given by  $\mathbf{T}_j = \mathbf{W}_0 \mathbf{W}_j^H$  where  $\mathbf{W}_0$  and  $\mathbf{W}_j$  are the unitary matrices in the polar decomposition of  $\mathbf{A}_0$  and  $\mathbf{A}_j$ . Thus, the focusing matrix (9) can be written as

$$\mathbf{T}_j = \mathbf{W}_0 \mathbf{W}_j^H \quad (10)$$

$$= \mathbf{W}_0 \mathbf{Q}_0 \mathbf{Q}_0^{-1} \mathbf{Q}_j^{-H} \mathbf{Q}_j^H \mathbf{W}_j^H \quad (11)$$

$$= \mathbf{A}_0 \mathbf{Q}_0^{-1} \mathbf{Q}_j^{-1} \mathbf{A}_j^H. \quad (12)$$

Since  $\mathbf{A}_0$  is full column rank, the positive-definite matrices  $\mathbf{Q}_0$  and  $\mathbf{Q}_j$  are uniquely determined by  $(\mathbf{A}_0^H \mathbf{A}_0)^{\frac{1}{2}}$  and  $(\mathbf{A}_j^H \mathbf{A}_j)^{\frac{1}{2}}$ . Thus, (12) is the same as

$$\mathbf{T}_j = \mathbf{A}_0 (\mathbf{A}_0^H \mathbf{A}_0)^{-\frac{1}{2}} (\mathbf{A}_j^H \mathbf{A}_j)^{-\frac{1}{2}} \mathbf{A}_j^H. \quad (13)$$

**Theorem 3.** *The perturbation errors in the least-square and the total least-square approaches are related by*

$$\frac{\|\mathbf{E}_0\|^2}{2} \leq \|\mathbf{F}_0\|^2 + \|\mathbf{F}_j\|^2 \leq \|\mathbf{E}_0\|^2 \quad (14)$$

with equality in the left hand side when  $\omega_j$  is equal to  $\omega_0$ .

This theorem indicates that the total least-square approach has a smaller error than the least-square method. Furthermore, the left inequality is tight specially in a neighborhood of the focusing frequency.

The computational complexity of the new method is due to square root computation and inversion of  $\hat{q} \times \hat{q}$  matrices  $\mathbf{A}_0^H \mathbf{A}_0$  and  $\mathbf{A}_j^H \mathbf{A}_j$ . It is important to note that the TLS algorithm does not require a singular value decomposition. In contrast to the TLS algorithm, the CSM needs a singular value decomposition of  $p \times p$  matrices. Usually  $\hat{q}$  is much smaller than  $p$  the number of sensors. And hence the computational complexity for the TLS formulation is significantly lower than that for the CSM algorithm.

## 4. Simulation results

In the first example, we consider a configuration with two wideband sources from the angles of arrival 10 and 14 degrees in the far field of a uniform linear array of 8 sensors. The spacing between each two consecutive sensors is half the wavelength at the center frequency of the spectrum of the wideband signals. The sources have the same complex frequency spectrum which is flat over a 40 percent relative bandwidth. The output of each sensor is decomposed into 100 snapshots of 32 samples each. An FFT algorithm is used in each snapshot to sample the spectrum of signals. A Monte-Carlo simulation is performed and the bias, the standard deviation, and the resolution are averaged over 200 independent runs. At each trial a delay-and-sum beamformer is used to estimate the DOAs. Then, two extra angles are added at 1 degree from the estimated DOA. This simulation was performed for different signal-to-noise ratios and

the bias and the standard deviation are reported in Table 1 and Table 2.

We have also compared the resolution of the CSM and the TLS methods. The resolution criterion is defined as the difference between the average of the spatial spectrum at the peak points in the MUSIC algorithm and the spatial spectrum in the valley. The result is shown in Fig. 1.

To find the resolution threshold, we ran 100 independent trials for different SNRs. Number of times that each algorithm resolved the sources was counted to estimate the probability of resolution. The sources were assumed to be resolved when two peaks in the spatial spectrum of the MUSIC algorithm were in the vicinity (within  $1^\circ$ ) of the true DOA. Fig. 2 shows the probability of the resolution for the two methods. It is seen that the resolution threshold for the TLS algorithm is smaller than that for the CSM.

To study the performance of the TLS algorithm for multi-group sources, we added two more sources at 33 and 37 degrees and increased the number of sensors to 20. Table 3 presents the results of average bias for 100 independent runs. As it is seen, the CSM and the TLS algorithms have a similar performance. Fig. 3 depicts the MUSIC spatial spectrum for this example for  $-15$  dB signal-to-noise ratio. For higher SNRs the two spectrum overlap. Note that the same performance as the unitary CSM has been achieved using the TLS algorithm with a smaller computational complexity.

## References

- [1] H. Wang and M. Kaveh, "Coherent signal-subspace processing for the detection and estimation of angles of arrival of multiple wide-band sources," *IEEE Trans. Acoust., Speech, Signal Processing*, vol. 33, pp. 823-831, August 1985.
- [2] H. Hung and M. Kaveh, "Focusing matrices for coherent signal-subspace processing," *IEEE Trans. Acoust., Speech, Signal Processing*, vol. 36, pp. 1272-1281, August 1988.
- [3] M. A. Doron and A. J. Weiss, "On focusing matrices for wide-band array processing," *IEEE Trans. Signal Processing*, vol. SP-40, pp. 1295-1292, June 1992.
- [4] H. Hung and M. Kaveh, "On the statistical sufficiency of the coherently averaged covariance matrix for the estimation of the parameters of wideband sources," in *proceeding IEEE Int. Conf. Acoust., Speech, Signal Processing*, 1987.
- [5] G. H. Golub and C. F. V. Loan, *Matrix Computations*. The Johns Hopkins University Press, 1983.
- [6] S. Valaee, B. Champagne, and P. Kabal, "Localization of wideband signals using a total least-square approach," submitted to *IEEE Trans. Signal Processing*, April 1994.
- [7] K. S. Arun, "A unitarily constrained total least squares problem in signal processing," *SIAM J. Matrix Anal. Appl.*, vol. 13, pp. 729-745, July 1992.

SNR	CSM		TLS	
	10	14	10	14
0	-0.0358	0.0324	-0.0054	-0.0012
10	0.0016	-0.0043	-0.0011	-0.0019
20	0.0046	-0.0062	-0.0003	-0.0011
30	0.0050	-0.0062	-0.0004	-0.0006
40	0.0051	-0.0061	-0.0001	-0.0009
50	0.0051	-0.0061	-0.0000	-0.0006

**Table 1** The average bias for 200 independent runs for a scenario with two closely separated sources at 10 and 14 degrees arriving at a uniform linear array of 8 sensors using the TLS and CSM algorithms.

SNR	CSM		TLS	
	10	14	10	14
0	0.1211	0.1354	0.1202	0.1310
10	0.0350	0.0392	0.0353	0.0386
20	0.0124	0.0143	0.0125	0.0139
30	0.0076	0.0090	0.0076	0.0084
40	0.0070	0.0083	0.0066	0.0076
50	0.0070	0.0083	0.0070	0.0077

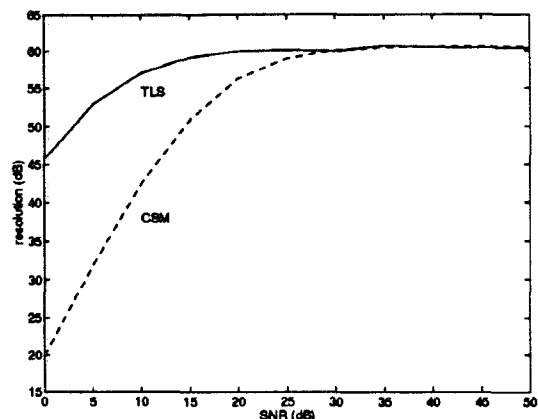
**Table 2** The average standard deviation for 200 independent runs for a scenario with two closely separated sources at 10 and 14 degrees arriving at a uniform linear array of 8 sensors using the TLS and CSM algorithms.

SNR	CSM			
	10	14	33	37
0	-0.0319	0.0417	-0.0340	0.0353
10	-0.0324	0.0402	-0.0330	0.0352
20	-0.0328	0.0405	-0.0330	0.0353
30	-0.0327	0.0403	-0.0331	0.0353
40	-0.0328	0.0402	-0.0332	0.0353
50	-0.0327	0.0402	-0.0332	0.0352

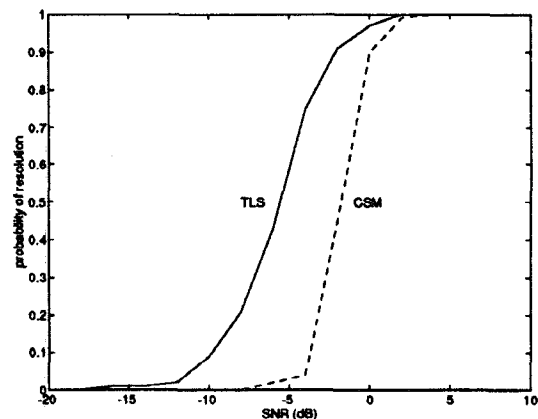
  

SNR	TLS			
	10	14	33	37
0	-0.0381	0.0370	-0.0146	0.0422
10	-0.0410	0.0357	-0.0159	0.0445
20	-0.0400	0.0337	-0.0146	0.0430
30	-0.0387	0.0346	-0.0149	0.0428
40	-0.0400	0.0348	-0.0152	0.0437
50	-0.0394	0.0320	-0.0146	0.0433

**Table 3** The average bias for 100 independent runs for a scenario with 4 closely separated sources at 10, 14, 33, and 37 degrees arriving at a uniform linear array of 20 sensors using the TLS and CSM algorithms.



**Fig. 1** The resolution of the TLS and CSM methods for a scenario with two closely separated sources at 10 and 14 degrees.



**Fig. 2** The probability of resolution for the TLS and CSM methods for a scenario with two closely separated sources at 10 and 14 degrees.

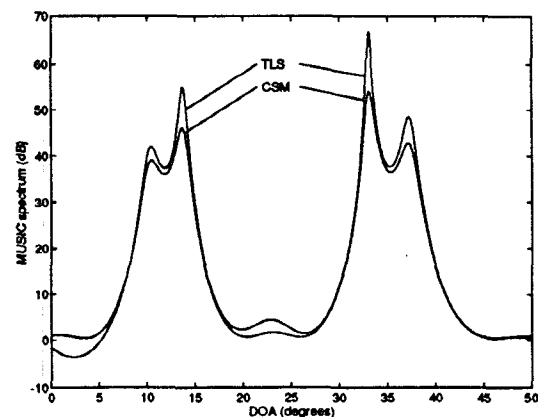


**Fig. 3** The MUSIC spectrum for a scenario with 4 equi-power wideband sources at 10, 14, 33, and 37 degrees arriving at a uniform linear array of 20 sensors.